

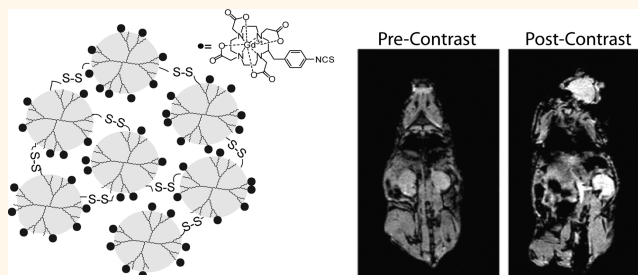
# Biodegradable Polydisulfide Dendrimer Nanoclusters as MRI Contrast Agents

Ching-Hui Huang,<sup>†</sup> Kido Nwe,<sup>‡</sup> Ajlan Al Zaki,<sup>†</sup> Martin W. Brechbiel,<sup>‡</sup> and Andrew Tsourkas<sup>†,\*</sup>

<sup>†</sup>Department of Bioengineering, School of Engineering and Applied Science, University of Pennsylvania, Philadelphia, Pennsylvania 19104, United States and

<sup>‡</sup>Radioimmune Inorganic Chemistry Section, National Cancer Institute, Bethesda, Maryland 20892, United States

**ABSTRACT** Gadolinium-conjugated dendrimer nanoclusters (DNCs) are a promising platform for the early detection of disease; however, their clinical utility is potentially limited due to safety concerns related to nephrogenic systemic fibrosis (NSF). In this paper, biodegradable DNCs were prepared with polydisulfide linkages between the individual dendrimers to facilitate excretion. Further, DNCs were labeled with premetalated Gd chelates to eliminate the risk of free Gd becoming entrapped in dendrimer cavities. The biodegradable polydisulfide DNCs possessed a circulation half-life of >1.6 h in mice and produced significant contrast enhancement in the abdominal aorta and kidneys for as long as 4 h. The DNCs were reduced in circulation as a result of thiol–disulfide exchange, and the degradation products were rapidly excreted *via* renal filtration. These agents demonstrated effective and prolonged *in vivo* contrast enhancement and yet minimized Gd tissue retention. Biodegradable polydisulfide DNCs represent a promising biodegradable macromolecular MRI contrast agent for magnetic resonance angiography and can potentially be further developed into target-specific MRI contrast agents.



**KEYWORDS:** gadolinium · magnetic resonance · nanoparticle · nanocluster · dendrimer · biodegradable

Magnetic resonance imaging (MRI) contrast agents are extensively being used to diagnose diseases by enhancing image contrast between pathological and normal tissues. Various paramagnetic compounds have been evaluated as MR contrast agents, but chelated gadolinium (Gd) compounds continue to be the most widely used. Clinically approved Gd-based contrast agents, such as Gd(III)-diethylenediaminepentaacetic acid ([Gd-(DTPA)]<sup>−2</sup>) (Magnevist) and Gd(III)-*N,N,N',N''*-tetracarboxymethyl-1,4,7,10-tetraazacyclododecane<sup>1,2</sup> ([Gd(DOTA)]<sup>−1</sup>) (Dotarem), have proven to be invaluable in diagnosing diseases such as cancer and multiple sclerosis and in enhancing MR angiographies. However, despite their utility, these agents suffer from poor sensitivity and rapid renal clearance, which severely limits the time window for MR imaging. As a result of these shortcomings, numerous macromolecular Gd(III)-appended agents have been developed not only to increase blood circulation time but also to enhance the longitudinal

relaxivities ( $r_1$ ) per gadolinium. Macromolecular gadolinium-based MRI contrast agents have been constructed by coupling chelated gadolinium complexes to polymers,<sup>3</sup> dendrimers,<sup>4</sup> vesicles,<sup>5,6</sup> proteins,<sup>7</sup> and other platforms.<sup>8</sup> Although macromolecular agents have demonstrated enhanced MR contrast and increased circulation time, their translation to the clinic has often been hampered by their slow and, in some cases, incomplete excretion.<sup>9–11</sup> A concern with slow excretion is that it may lead to an increase in tissue accumulation and transmetalation of chelated Gd, thus increasing the possibility of toxic side effects and the onset of nephrogenic systemic fibrosis (NSF).<sup>12</sup>

Recent efforts to develop macromolecular gadolinium-based MRI contrast agents have focused on introducing biodegradable materials and/or linkages into the design.<sup>8,13,14</sup> Biodegradable macromolecular agents maintain the ability to carry high payloads of gadolinium and are large enough to prolong the blood circulation time; however, following intravenous administration, they

\* Address correspondence to atsourk@seas.upenn.edu.

Received for review April 3, 2012 and accepted October 25, 2012.

Published online October 25, 2012  
10.1021/nn304160p

© 2012 American Chemical Society

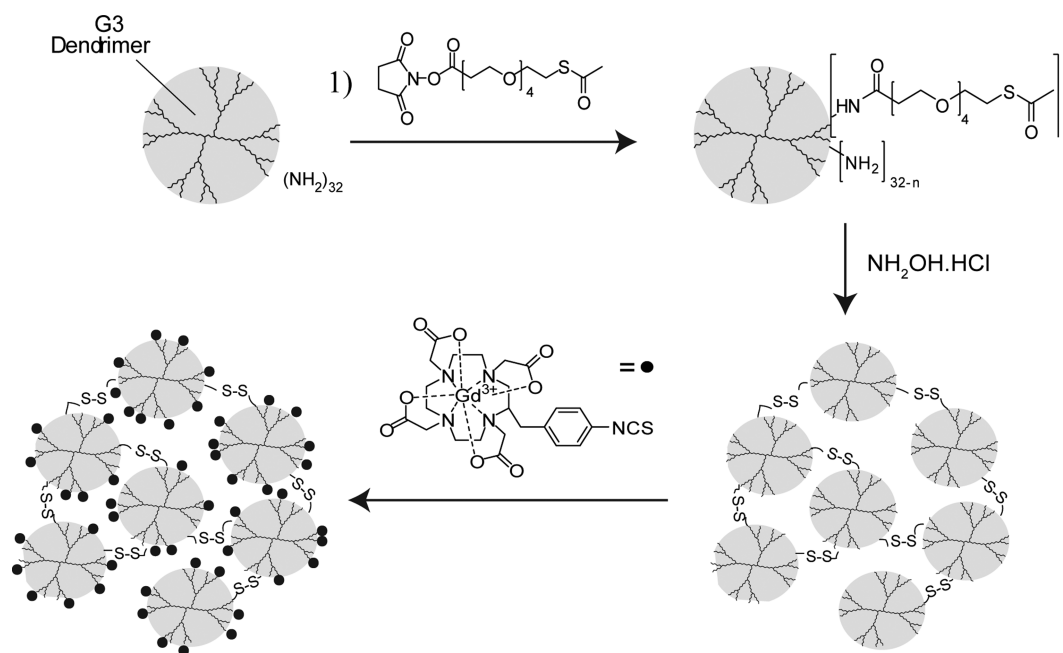


**Figure 1.** Schematic illustrating the synthetic approach used to prepare gadolinium (Gd)-labeled polydisulfide dendrimer nanoclusters (DNCs). PAMAM dendrimers (G3) were first reacted with SAT(PEG)<sub>4</sub>. The thiolated dendrimers were then suspended in an alkaline buffer for deprotection and to initiate the formation of polydisulfide DNCs. Once DNCs with a desirable hydrodynamic diameter were formed, free thiols were quenched with maleimide and the remaining amines were functionalized with [Gd-C-DOTA]<sup>-1</sup>.

are degraded into smaller molecular species that can be readily excreted. The strategy for the design of biodegradable agents generally involves integrating acid-labile or redox-responsive bonds into the macromolecular structure. Acid-labile biodegradability is based on the *in vivo* lability of designated bonds<sup>15</sup> in the presence of an acidic environment, whereas redox-responsive biodegradability is based on the *in vivo* thiol exchange of disulfide bonds in the presence of endogenous thiols.<sup>16</sup>

We have recently reported gadolinium-conjugated dendrimer nanoclusters (DNCs) as  $T_1$  MRI contrast agents.<sup>17</sup> DNCs are composed of individual gadolinium-labeled poly(amido amine) (PAMAM) dendrimers that have been cross-linked to form larger nanoparticulate carriers. Gadolinium-conjugated DNCs demonstrated site-specific targeting and significant contrast enhancement. In this paper, we modified the design of DNCs to include polydisulfide linkages between the individual dendrimers. These biodegradable polydisulfide DNCs inherit the high relaxivity of DNCs and retain an extended circulation time but are reduced to smaller degradation products while in circulation and undergo efficient renal excretion, reducing the possibility of long-term macromolecular particle retention.

## RESULTS

**Synthesis and Characterization of Polydisulfide DNCs.** A schematic illustrating the approach used to synthesize biodegradable polydisulfide DNCs is presented in Figure 1. The polydisulfide DNCs were prepared by first

attaching *N*-succinimidyl (*S*)-acetyl(thiotetraethylene glycol) (SAT(PEG)<sub>4</sub>) to PAMAM (generation 3; G3) dendrimers. Prior to modification, PAMAM(G3) dendrimers have a diameter of  $\sim 3.6$  nm. The use of a polyethylene glycol (PEG) spacer arm increased the water solubility of the thiolated dendrimers. It was determined by elemental analysis that approximately 13 thiol groups were incorporated onto each PAMAM(G3) dendrimer. Consequently, 19 of the 32 primary amines per PAMAM(G3) dendrimer remained active for downstream labeling with premetallated Gd chelates. The formation of polydisulfide cross-linked nanoclusters was initiated by deprotecting the thiol groups on the thiolated dendrimers in PBS at room temperature. The change in the mean hydrodynamic diameter of the nanoclusters was then monitored by dynamic light scattering (DLS, Figure 2A) and stopped once a desirable size was achieved, by quenching all of the remaining free thiols through the addition of excess maleimide. Representative size distributions of various nanoclusters obtained over the course of a reaction are shown in Figure 2B. The nanoclusters were subsequently labeled with Gd by reacting the amine functional groups with premetallated 2-(4-isothiocyanatobenzyl)-1,4,7,10-tetraazacyclododecane-*N,N',N'',N'''*-tetraacetic acid gadolinium complexes ([Gd-C-DOTA]<sup>-1</sup>).<sup>18</sup> No substantial change in the hydrodynamic diameter of the DNCs was observed after conjugation of the gadolinium complexes.

Polydisulfide DNCs with three distinct hydrodynamic diameters, 59, 91, and 142 nm as measured

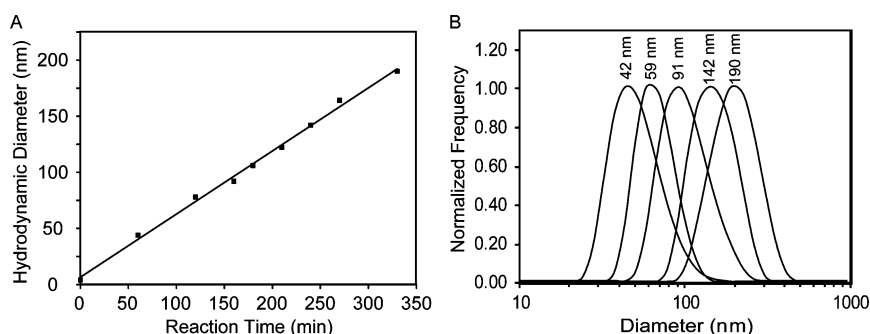


**Figure 2.** Dynamic light scattering (DLS) analysis of DNCs. (A) Thiol-functionalized PAMAM(G3) dendrimers were incubated in alkaline buffer, and the mean hydrodynamic diameter of the resulting nanoclusters was monitored as a function of time. (B) Representative hydrodynamic size distributions of polysulfide DNCs. All DNCs possessed a PDI < 0.2.

**TABLE 1.** Physical and Magnetic Properties of DNCs

size (nm)	relaxivity ( $r_1$ , $\text{mM}^{-1} \text{s}^{-1}$ )	zeta-potential <sup>a</sup> ( $\zeta$ , mV)
59	11.7	-9.5
91	18.4	-13.4
142	22.4	-5.4

<sup>a</sup>Zeta-potential describes the electrokinetic potential in colloidal systems, which does not necessarily correlate with particle size.

by DLS, were chosen for further study and characterization. Transmission electron microscopy (TEM) images indicated that the selected DNCs were approximately spherical in shape, particularly the two smaller fractions, and had average physical diameters of  $52 \pm 17$ ,  $86 \pm 21$ , and  $121 \pm 10$  nm, respectively (Figure S1 in the Supporting Information).

**Molar Relaxivity of Polydisulfide DNCs.** The concentration of Gd within the three selected polydisulfide DNC samples was determined by inductively coupled plasma mass spectroscopy (ICP-MS). The relaxivities ( $r_1$ ) were then determined by plotting the inverse of longitudinal relaxation time ( $1/T_1$ ) as a function of gadolinium concentration (Figure S2). The 59, 91, and 142 nm polydisulfide DNCs had  $r_1$  values of 11.7, 18.4, and  $22.4 \text{ mM}^{-1} \text{ s}^{-1}$  per gadolinium ion, respectively. It is likely that the increase in relaxivity with size can primarily be attributed to an increase in the rotational correlation time ( $\tau_c$ ) of the chelated Gd; however, changes in the inner-sphere water exchange rate and the internal motion of the polydisulfide DNC will also influence the measured relaxivities.<sup>19–22</sup> The DNC relaxivity values are greater than that of Gd-DOTA ( $r_1 = 3.9 \text{ mM}^{-1} \text{ s}^{-1}$ ) and PAMAM(G3)-[Gd-C-DOTA]<sup>-1</sup> ( $r_1 = 10.9 \text{ mM}^{-1} \text{ s}^{-1}$ ). The values of relaxivity and zeta-potential ( $\zeta$ , mV) of the various polydisulfide DNCs are summarized in Table 1.

The number of premetalated Gd-DOTA complexes per 59 nm polydisulfide DNC was calculated by using the viscosity/light-scattering method<sup>23</sup> in combination with ICP-MS. The viscosity/light-scattering method utilizes Einstein's viscosity equation to solve for the volume fraction of DNCs. This value is then divided by the average nanoparticle volume, obtained from

dynamic light scattering, to acquire the concentration of DNCs in a sample. ICP-MS is then used to determine the Gd concentration of the sample, and thus the number of Gd per DNC can be readily determined. Measurements of Gd-DOTA per DNC were limited to the 59 nm formulation because of the high concentrations ( $\sim 20 \text{ mM}$  Gd) and volumes (1 mL per measurement, 5 measurements) needed for accurate viscosity measurements. For similar reasons, only the 59 nm DNC was selected for *in vivo* evaluation. The viscosity/light-scattering method in combination with ICP-MS indicated that there were approximately 9400 premetalated [Gd-C-DOTA]<sup>-1</sup> per 59 nm polydisulfide DNC particle. This infers an  $r_1$  per polydisulfide DNC of  $109\,980 \text{ mM}^{-1} \text{ s}^{-1}$ . Higher relaxivities/payloads can presumably be achieved by selecting a polydisulfide DNC with a larger hydrodynamic diameter or potentially by adopting higher generation dendrimers to increase the number of surface functional groups. Notably, synthesis of polydisulfide DNCs composed of higher generation dendrimers (G5) was attempted, but poor solubility during the cross-linking step prohibited their use.

**Degradability of Polydisulfide DNCs in the Presence of Thiols and Stability at Various pH Values.** The degradability of polydisulfide DNCs in serum was modeled by incubating DNCs in the presence of thiols that are normally found in human and rat plasma and measuring hydrodynamic diameter as a function of time. Surprisingly, the polydisulfide DNCs remained stable for at least 24 h. Representative results of 59 nm DNCs in mock human serum are shown in Figure 3A; however, there was no noticeable difference for DNCs with various hydrodynamic diameters or between DNCs incubated in rat or human thiol mixtures. Upon the addition of dithiothreitol (DTT) at 24 h, all of the DNC formulations were immediately reduced to less than 10 nm. Similar results were observed when DTT was added to DNCs suspended in phosphate buffered saline (PBS). The unexpected stability of the DNCs in the presence of endogenous thiols could be the result of steric hindrance or charge repulsion at the [Gd-C-DOTA]<sup>-1</sup>-conjugated nanocluster surface, which may have

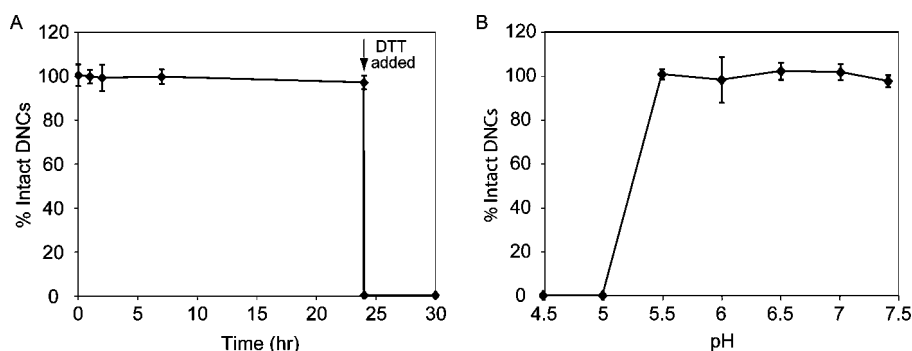


**Figure 3.** Stability of polydisulfide DNCs in the presence of thiols and at various pH. Polydisulfide DNCs (0.5 mM Gd) were incubated with a mixture of thiols that reflected the thiol content found in human plasma (10  $\mu$ M cysteine, 5  $\mu$ M glutathione, 3  $\mu$ M cysteinylglycine). (A) Stability of DNCs in the presence of the thiol mixture was determined by measuring the hydrodynamic diameter on DLS over the course of 24 h. After 24 h, DTT (50  $\mu$ M) was added to the sample to confirm that the polydisulfide linkages within DNCs were susceptible to a reducing agent. (B) Stability of polydisulfide DNCs was also examined as a function of pH. The polydisulfide DNCs were added in buffered solutions at various pH, and the hydrodynamic diameter was measured after 1 h by DLS.

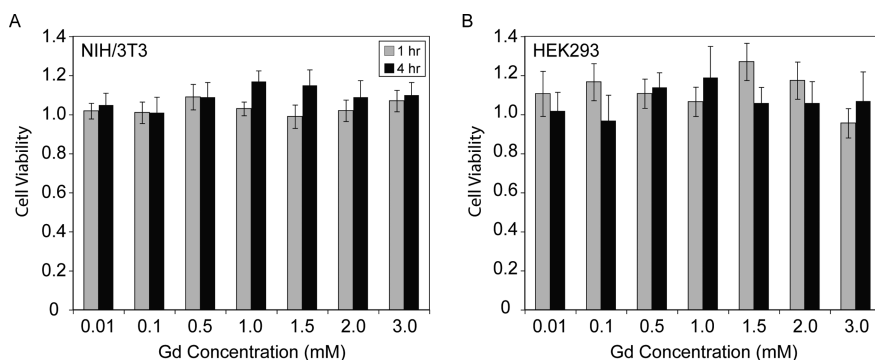


**Figure 4.** Cell viability of NIH/3T3 and HEK 293 cells following incubation with polydisulfide DNCs. Gd-labeled polydisulfide DNCs were incubated with NIH 3T3 and HEK 293 cells at various Gd concentrations for 1 or 4 h. Cell viability was measured using an MTT assay and normalized to cells in the absence of any polydisulfide DNCs.

prohibited the endogenous thiols from entering the nanoclusters. Potentially, only small molecules, such as DTT, can reach the disulfide bonds for the thiol–disulfide exchange to occur.

The stability of three polydisulfide DNCs was also tested at various pH, ranging from 4.5 to 7.5. A dramatic loss of intact DNCs was observed at pH values below 5.5 (Figure 3B), which indicates that polydisulfide DNCs are unstable in acidic environments. The destabilization of polydisulfide DNCs at pH values below 5.5 occurred instantly. For example, at pH 5.0, only ~18% of the polydisulfide DNCs remained intact after 5 min, and no intact DNCs were observed after 30 min (Figure S3). At lower pH values, no intact DNCs were observed even after just 5 min.

**Cytotoxicity of Polydisulfide DNCs.** The toxicity of 59 nm polydisulfide DNCs was examined *via* an MTT (3-(4,5-dimethylthiazol-2-yl)2,5-diphenyltetrazolium bromide) cell proliferation assay. Various concentrations of polydisulfide DNCs were incubated with NIH 3T3 fibroblasts and human embryonic kidney (HEK) 293 cells for 1 and 4 h. The results shown in Figure 4 were normalized to a control cell sample incubated without polydisulfide DNCs. In general, polydisulfide DNCs did

not show any significant effect on cell proliferation at gadolinium concentrations up to 3 mM. Additional MTT assays were also performed at 24 and 48 h with Gd concentrations up to 1 mM (Figure S4). Under these conditions, DNCs again did not exhibit any inhibitory effect on the proliferation of NIH/3T3 and HEK293 cells.

**Pharmacokinetics of Polydisulfide DNCs.** The circulation time of polydisulfide DNCs (59 nm) in nude mice was evaluated by measuring the gadolinium concentration in blood over the course of 24 h *via* ICP-MS (Figure 5A). It was determined that the half-life ( $t_{1/2}$ ) for the initial elimination phase of DNCs from the blood was approximately 1.6 h, which was obtained by fitting the first 6 h of data. This is considerably longer than that of generation 3 (G3) PAMAM dendrimers ( $t_{1/2} < 15$  min)<sup>24,25</sup> and other macromolecular gadolinium-based contrast agents (such as cysteine-based copolymers,  $t_{1/2} < 1$  h).<sup>14,26,27</sup> For comparison, less than 1% injected dose (I.D.) of PAMAM(G3) dendrimer per gram blood remained in circulation after just 1 h post-injection. In contrast, 13.6% I.D. of polydisulfide DNCs per gram blood was still in circulation after 1 h, and more than 1% I.D./gram was still present 6 h after intravenous administration.

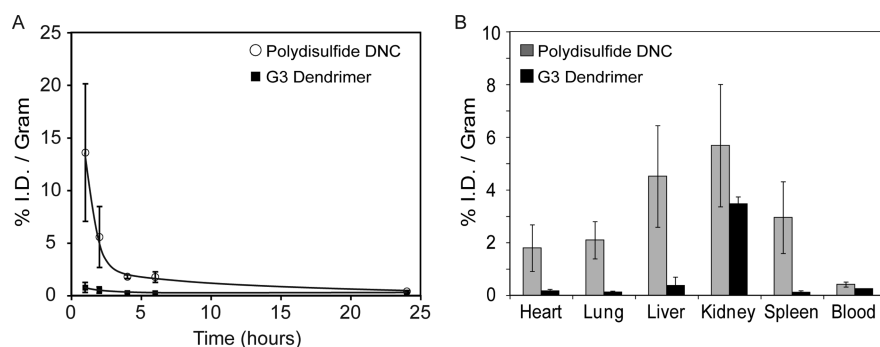


**Figure 5.** Blood clearance and biodistribution of polydisulfide DNCs and PAMAM(G3)-[Gd-C-DOTA]<sup>-1</sup>. Polydisulfide DNCs (59 nm) and PAMAM(G3)-[Gd-C-DOTA]<sup>-1</sup> (3.6 nm) were administered intravenously into nu/nu mice ( $n = 3$  each). (A) Blood samples were collected at various time points post-injection and analyzed for Gd content *via* ICP-MS. (B) Mice were sacrificed 24 h following the administration of contrast agents, and select organs were harvested and also analyzed for Gd content.

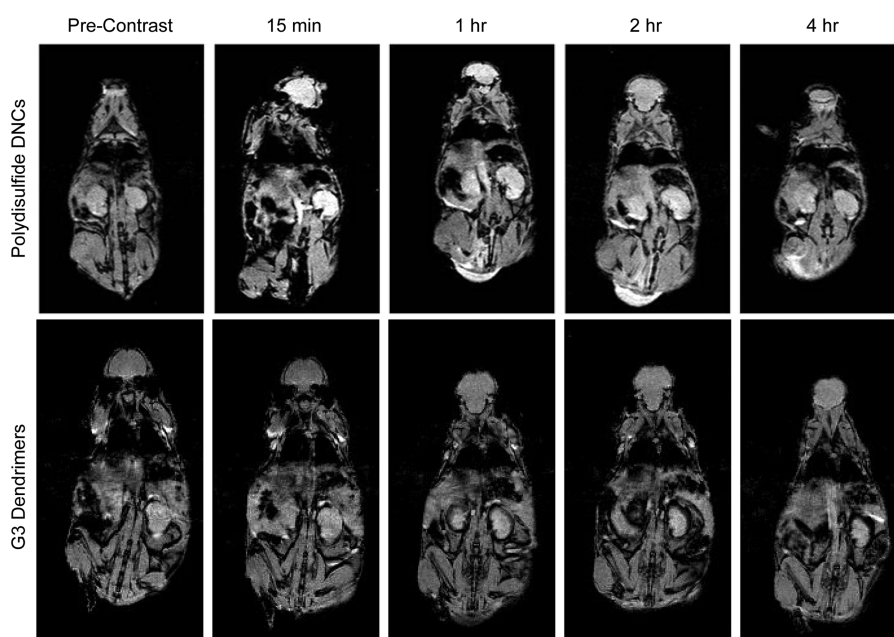


**Figure 6.** Magnetic resonance images of nu/nu nude mice at various time points after the tail vein injection of polydisulfide DNCs or PAMAM(G3)-[Gd-C-DOTA]<sup>-1</sup>.  $T_1$ -weighted mages of the kidney were acquired pre-injection and 15 min, 1 h, 2 h, and 4 h post-injection. All images were acquired using a 4.7 T small animal horizontal bore Varian INOVA system.

The accumulation of gadolinium in the heart, lung, liver, kidney, spleen, and blood of the mice was examined 24 h post-injection (Figure 5B). Overall, the accumulation of gadolinium was modest in all of the organs examined, with the highest uptake observed in the kidney ( $5.68 \pm 2.32\%$  I.D./g) followed by liver ( $4.52 \pm 1.93\%$  I.D./g) and then the spleen ( $2.95 \pm 1.36\%$  I.D./g). The biodistribution of polydisulfide DNCs did exhibit a higher accumulation of Gd within each of the organs evaluated, compared with individual PAMAM-(G3) dendrimers, but uptake was substantially lower than what has been reported for higher generation dendrimers. For example, PAMAM(G6)-OH (6.7 nm) has a liver uptake of  $\sim 40\%$  I.D./g and a kidney uptake of  $\sim 20\%$  I.D./g at 24 h post-injection.<sup>28</sup> The organ uptake of DNCs was likely lower than PAMAM(G6)-OH owing to its ability to degrade into smaller molecular

species that are more efficiently cleared by renal filtration.

***In Vivo* MRI Contrast Enhancement.** To investigate the MR contrast enhancing capabilities of DNCs (59 nm),  $T_1$ -weighted MR images of nude mice were acquired pre-injection, and 15 min, 1 h, 2 h, and 4 h post-injection (Figure 6). A significant contrast enhancement in  $T_1$ -weighted images was clearly visible in the kidneys and abdominal aorta at 15 min and 1 h post-injection. Quantitative analysis revealed a statistically significant ( $p < 0.5$ ) enhancement in the kidneys for as long as 4 h (Figure S5).  $T_1$ -weighted images of mice injected with PAMAM(G3)-[Gd-C-DOTA]<sup>-1</sup> did not reveal any enhancement in the kidneys at any of the time points studied, which is consistent with rapid clearance from the body. Only a slight signal enhancement was found in the bladder at 15 min post-injection



of DNCs (Figure S6), but a gradual increase in signal was observed over the next 4 h. These biodistribution trends provide strong evidence that gadolinium is being cleared *via* renal filtration following the intravenous administration of DNCs.

## DISCUSSION

The ideal MR contrast agents should greatly enhance image contrast and provide a sufficient time window for MR examination. Furthermore, the agents should be excreted rapidly following the acquisition of MR images. In order to enhance image contrast and prolong the time window for MR acquisition, our group previously developed gadolinium-conjugated dendrimer nanoclusters as MR imaging contrast agents.<sup>17</sup> The first iteration of this nanoparticle design performed well but did not include any acid-labile or redox-responsive biodegradable elements to facilitate their degradation and excretion. Further, a relatively unstable linear chelate, DTPA, was used to complex Gd to the nanocluster. With an expanding body of literature linking Gd to nephrogenic systemic fibrosis (NSF) in patients with impaired renal function, it is becoming increasingly evident that Gd-based imaging agents must strike a delicate balance between providing an extended time frame for imaging and possessing the ability to be rapidly excreted from the body. Further, stable chemical chelators must be used to minimize the possibility of transmetalation of Gd. Therefore, the polydisulfide DNCs presented in this paper were specifically designed to incorporate biodegradable linkages between individual PAMAM(G3) dendrimers, and Gd was complexed to the DNCs using a stable, macrocyclic chelator, DOTA.

The formation of biodegradable DNCs was initiated by removing the protecting groups from thiols that were sparingly introduced onto PAMAM(G3) dendrimers. The size of dendrimer nanoclusters was then easily controlled by adding an excess of maleimide to the reaction at different time points to quench the free thiols and stop disulfide bond formation. Since the hydrodynamic diameter of the nanoclusters increased slowly and could be readily monitored *via* DLS, nanoparticles with nearly any size and with narrow size distributions could be obtained. DNCs were subsequently labeled with the premetalated gadolinium complex  $[\text{Gd-C-DOTA}]^{-1}$ .

To date, most macromolecular gadolinium complexes have used the linear ligand DTPA as a chelation agent. However, with recent reports suggesting that transmetalation of Gd is the major factor contributing to NSF for patients with compromised kidney function,<sup>29–31</sup> it is speculated that a macrocyclic chelator would provide a more stable and safer alternative. Supporting this notion are findings that NSF has almost exclusively been linked to linear Gd chelates, and there are no reported cases of NSF in patients that received

$[\text{Gd(DOTA)}]^{-1}$ /gadoterate/Dotarem.<sup>32</sup>  $[\text{Gd(DOTA)}]^{-1}$  is known to be more stable in comparison to  $[\text{Gd(DTPA)}]^{-2}$ , with 5 orders of magnitude higher stability *in vitro* and an exceedingly slow metal ion dissociation even at very low pH.<sup>33</sup> The use of  $[\text{Gd-C-DOTA}]^{-1}$ , which has Gd complexed with DOTA prior to labeling the dendrimers (*i.e.*, premetalation), further reduces concerns over toxicity. When dendrimers are labeled with Gd after reacting the dendrimer with a chelator (*i.e.*, postmetalation), free gadolinium ions can potentially become trapped within dendrimer cavities. Others have shown that cavities of dendrimers are capable of encapsulating small molecules.<sup>34</sup> In cases where this is not desirable, free Gd ions can be removed through extensive purification; however, the premetalation of  $[\text{Gd-C-DOTA}]^{-1}$  in this study greatly alleviates concerns over incomplete purification.

Previously, we reported that gadolinium-conjugated DNCs<sup>17</sup> (~150 nm) could be labeled with approximately 300 000 gadolinium ions per DNC and possessed an  $r_1$  of  $3.6 \times 10^6 \text{ mM}^{-1} \text{ s}^{-1}$  (per DNC). Here, it was determined that there were approximately 9400 premetalated  $[\text{Gd-C-DOTA}]^{-1}$  per 59 nm polydisulfide DNC. Scaling with volume, it can be estimated that there would be approximately 150 000 Gd per 150 nm polydisulfide DNC particle and each DNC would have an  $r_1$  of  $3.4 \times 10^6 \text{ mM}^{-1} \text{ s}^{-1}$ , assuming a relaxivity of  $22.4 \text{ mM}^{-1} \text{ s}^{-1}$  per gadolinium ion. The slightly lower payload is likely the result of there being fewer functional groups per dendrimer, due to prior labeling with SAT(PEG)<sub>4</sub> and/or the use of lower generation dendrimers, G3 *versus* G5. Notably, the  $r_1$  per Gd was higher for the ~150 nm polydisulfide DNCs compared with the prior formulation. This stems from the use of premetalated  $[\text{Gd-C-DOTA}]^{-1}$ , which has been previously shown to lead to improved  $r_1$  values compared with postmetalation methods.<sup>18</sup> For further comparison, the  $r_1$  (per Gd) of other polydisulfide gadolinium complexes that have been reported for use as blood pool agents ranges from  $4.4$  to  $16.3 \text{ mM}^{-1} \text{ s}^{-1}$ .<sup>13,35,36</sup>

Biodegradable agents are usually designed to break down into small molecular components under specific conditions such as a change in pH or a redox environment. The present biodegradable MRI contrast agents degrade *via* a thiol–disulfide exchange reaction in serum.<sup>8,14</sup> Interestingly, while the DNCs did degrade in serum, consistent with reports of other Gd-labeled polydisulfide macromolecules and nanoparticles,<sup>8,13,14</sup> they remained stable in the presence of freshly prepared thiol mixtures *in vitro*. This was somewhat surprising since the mixtures were specifically created to reflect the thiol content found in human and rat serum. The stability toward the thiol mixtures could be a result of steric hindrance or charge repulsion at the nanoclusters' surface, which may prevent the exchange reaction. This would be consistent with previous reports that found that the degradation rate of

polydisulfide gadolinium complexes decreased as the structural hindrance increased and as the size of the endogeneous thiols increased.<sup>14,35</sup> It is speculated that these steric effects may have been relaxed in actual serum due to the presence of other biomolecules that shielded the surface charges and enhanced DNC permeability.

Contrast-enhanced  $T_1$  weight images and biodistribution data suggested that the polydisulfide DNCs were gradually degraded in the blood circulation and were primarily excreted *via* renal filtration. Specifically, signal intensity was gradually enhanced in the bladder over the first 4 h, which is indicative of renal clearance. Further, the accumulation of gadolinium was highest in the kidneys. Since intact DNCs (59 nm) are too large to pass through the fenestrae in the capillaries of the glomeruli, which have a physiologic upper pore size limit of 15 nm,<sup>37</sup> it is likely that they were degraded into smaller clusters and/or individual dendrimers while in circulation. Individual gadolinium-labeled dendrimers (G3) have a hydrodynamic diameter of  $\sim 3.6$  nm and are readily excreted by glomerular filtration.<sup>24,26,27,38</sup>

Notably, despite the ability of polydisulfide DNCs to gradually degrade into smaller components in serum and be cleared *via* renal filtration, the bright image contrast observed in the abdominal aorta for the first hour after injection indicated that polydisulfide DNCs exhibit a prolonged blood circulation time and can potentially be used as vascular contrast agents.

Polydisulfide DNCs demonstrated an excellent half-life ( $t_{1/2} > 1.6$  h) in comparison to individual gadolinium-based PAMAM dendrimers and other polydisulfide macromolecular contrast agents.<sup>14,26,27</sup> The significant difference in circulation time between polydisulfide DNCs and individual G3-PAMAM dendrimers suggests that polydisulfide DNCs do not degrade immediately after injection. To our knowledge, polydisulfide DNCs exhibit the longest half-life *in vivo* among all of the polydisulfide based  $T_1$  contrast agents reported to date.

## CONCLUSION

The use of polydisulfide-based gadolinium complexes as biodegradable macromolecular MRI contrast agents has garnered increasing interest in recent years. In our study, we have provided a facile method for the synthesis of size-controllable and biodegradable dendrimer nanoclusters. The polydisulfide DNCs provide long blood circulation times and gradually degrade into smaller components under physiological conditions, which greatly facilitates their renal clearance. The premetalated gadolinium DOTA complexes adopted in this study further alleviate the increasing concern over gadolinium-mediated toxicity. Further, future efforts can be made to develop polydisulfide DNCs into molecular imaging agents by conjugating appropriate targeting ligands. In conclusion, we believe that polydisulfide DNCs demonstrate great potential for clinical applications.

## METHODS

**Materials.** Poly(amido amine) (PAMAM) dendrimer (ethylene-diamine core, generation 3, 12% w/w in MeOH) was purchased from Dendritech Inc. SAT(PEG)<sub>4</sub> (*N*-succinimidyl (*S*)-acetyl(thiotetraethylene glycol)) was purchased from Quanta Biodesign Ltd. (Powell, OH). NIH/3T3 mouse fibroblasts were purchased from the American Type Culture Collection (ATCC, Manassas, VA). All other chemicals were purchased from Sigma-Aldrich (St. Louis, MO) unless otherwise noted.

**Synthesis of Premetalated Gadolinium Complexes ([Gd-C-DOTA]<sup>-1</sup>).** [Gd-C-DOTA]<sup>-1</sup> was synthesized as previously described.<sup>39</sup> Free Gd was removed from the [Gd-C-DOTA]<sup>-1</sup> sample using a Sephadex G-25 column (Pharmacia, Sweden). Complete removal of free Gd was confirmed by size-exclusion HPLC (SE-HPLC). SE-HPLC was performed using a Beckman System Gold (Fullerton, CA) equipped with model 126 solvent delivery module and a model 166NMP UV detector ( $\lambda$  254 nm) controlled by 32 Karat software. Size-exclusion chromatography was performed on a TSK-gel G3000PW 10  $\mu$ m, 7.8 mm  $\times$  300 mm (Tosoh Bioscience, Montgomeryville, PA), with a TSK-gel 10  $\mu$ m guard column (Tosoh Bioscience, Montgomeryville, PA) using phosphate buffered saline (1  $\times$  PBS) solution as the eluent at 1.0 mL/min, respectively.

**Synthesis of Gd-Labeled Polydisulfide Dendrimer Nanoclusters (DNCs).** Five microliters of *N,N*-diisopropylethylamine (DIEA) and 35  $\mu$ L of SAT(PEG)<sub>4</sub> (0.5 M in DMSO) were added to 100  $\mu$ L of PAMAM(G3) in 100  $\mu$ L of MeOH. Samples were mixed using a thermomixer (Eppendorf) at 1400 rpm, 25  $^{\circ}$ C, for 70 min. Ether was added until the solution turned cloudy, and thiolated dendrimers were collected by centrifugation (14 000 rpm, 10 min). Two more MeOH/ether washes were performed to remove any unreacted materials. Elemental analysis of the thiolated dendrimer indicated 49.09% C, 8.19% H, 14.62% N, and 3.65% S,

which is consistent with the incorporation of 13 thiol groups onto each PAMAM(G3) dendrimer, C<sub>471</sub>H<sub>307</sub>N<sub>122</sub>O<sub>136</sub>S<sub>13</sub> · 14HCO<sub>3</sub> · 10H<sub>2</sub>O: 48.84% C, 7.87% H, 14.33% N, and 3.50% S. The thiolated dendrimers were dissolved in 1 mL of PBS; NH<sub>2</sub>OH (1.5  $\times$  10<sup>-5</sup> mol) was added for deprotection, and the mixtures were stirred at room temperature. The cross-linking reaction was monitored by dynamic light scattering (DLS) using a Zetasizer Nano-ZS (Malvern Instruments, Worcestershire, UK). Once the desired particle size was obtained, maleimide (1.5  $\times$  10<sup>-5</sup> mol) was added to quench the reaction by blocking any remaining free thiols. The cross-linked dendrimers were dissolved in 20 mL of conjugation buffer (0.48 M NaHCO<sub>3</sub>, 0.02 M Na<sub>2</sub>CO<sub>3</sub>, 1.5 M NaCl, and 0.005 M EDTA), and 0.05 g premetalated [Gd-C-DOTA]<sup>-1</sup> was added in portions while the pH was maintained at 8.5 with 1 M NaOH. The mixture was stirred at 45  $^{\circ}$ C for 2 days. The solution was cooled to room temperature and filtered through a 0.22  $\mu$ m membrane filter. The solvent volume was reduced under high vacuum. The polydisulfide DNCs were purified by Sephadex G-25 columns, eluted with PBS. The first orange band was collected. To ensure the removal of unreacted premetalated [Gd-C-DOTA]<sup>-1</sup>, the Sephadex G-25 column was applied twice.

**Synthesis of PAMAM(G3)–[Gd-C-DOTA]<sup>-1</sup>.** PAMAM(G3)–[Gd-C-DOTA]<sup>-1</sup> was synthesized by conjugation of PAMAM(G3) dendrimer with premetalated [Gd-C-DOTA]<sup>-1</sup> according to the reported method.<sup>40</sup> Elemental analysis indicated 42.31% C, 6.01% H, 13.66% N, and 1.81% S, which is consistent with the incorporation of 10 chelates, C<sub>302</sub>H<sub>608</sub>N<sub>122</sub>O<sub>60</sub> · 10(C<sub>24</sub>H<sub>33</sub>N<sub>5</sub>O<sub>8</sub>S<sub>1</sub>Gd<sub>1</sub>) · 43HCO<sub>3</sub> · 6H<sub>2</sub>O: 41.99% C, 5.98% H, 14.04% N, and 1.92% S.

**Physicochemical Characterization of Polydisulfide DNCs.** The hydrodynamic diameter of DNCs was determined by DLS using a Zetasizer Nano-ZS (Malvern Instruments). The scattering angle

was set at 173°. Zeta-potential ( $\zeta$ ) measurements of DNCs were performed using the same instrument. All measurements were made in PBS.  $T_1$  relaxation times for polydisulfide DNCs, PAMAM(G3)-[Gd-C-DOTA] $^{-1}$ , and Gd-DOTA were determined with a Bruker mq60 MR relaxometer operating at 1.41 T (60 MHz) and 40 °C. Gadolinium concentration was determined by ICP-MS analysis using an Elan 6100 ICP-MS (Perkin-Elmer, Shelton, CT) at the New Bolton Center Toxicology Laboratory, University of Pennsylvania, School of Veterinary Medicine, Kennett Square, PA, USA. Transmission electron microscopy (TEM) was performed on a JEOL 2010 electron microscope. Elemental analysis was performed on C, H, N, and S by Intertek.

The number of Gd per DNC was determined using the viscosity/light-scattering method in combination with ICP-MS.<sup>23</sup> Specifically, the viscosity was first measured for wide range of DNC concentrations (0 to ~20 mM). The volume fraction ( $\phi$ ) of the DNCs was then determined according to Einstein's viscosity equation,  $h/h_0 = 1 + 2.5\phi$ , where  $h$  is the viscosity of the DNC suspension and  $h_0$  is the viscosity of the solvent. The number of DNCs per volume ( $N$ ) was obtained according to the equation  $N = \phi/[4/3\pi(d/2)^3]$ , where  $d$  is the volume-weighted diameter of DNCs, which was obtained by DLS. The concentration of Gd in the sample was determined by ICP-MS, which allowed for the calculation of Gd per DNC.

**DNC Degradation and Stability Studies.** Degradation of polydisulfide DNCs was evaluated by incubating DNCs (0.5 mM Gd, in PBS) with mixtures of thiols that are normally found in human and rat plasma. Specifically, solutions representing human plasma contained 10  $\mu$ M cysteine, 5  $\mu$ M glutathione, and 3  $\mu$ M cysteinylglycine, and solutions representing rat plasma contained 57  $\mu$ M cysteine and 26  $\mu$ M glutathione.<sup>41</sup> The degradation of polydisulfide DNCs in the presence of endogenous thiols was evaluated by monitoring changes in the hydrodynamic diameter by dynamic light scattering (DLS), using a Zetasizer Nano-ZS (Malvern Instruments, Worcestershire, UK), over the course of 24 h. The percent intact DNCs was calculated using the mean DLS diameter of DNCs in PBS as the reference. The stability of polydisulfide DNCs at various pH (4.5 to 7.5) was also evaluated by DLS over the course of 24 h. The polydisulfide DNCs were added to buffered pH solutions to achieve a final concentration of 0.5 mM Gd.

**Cell Culture.** NIH/3T3 mouse fibroblasts and human embryonic kidney 293 cells (HEK293) were cultured and maintained in Dulbecco's modified Eagle's medium (DMEM) with 10% fetal bovine serum (FBS), 1% penicillin/streptomycin at 37 °C and 5% CO<sub>2</sub>.

**Cell Viability Study.** The *in vitro* cytotoxicity of Gd-labeled polydisulfide DNCs was assayed with an MTT cell viability kit (ATCC, Manassas, VA). Specifically, NIH/3T3 and HEK293 cells were seeded in a 96-well plate at a density of  $4 \times 10^4$  cells per well and incubated overnight (37 °C, 5% CO<sub>2</sub>). The medium was aspirated off, and 100  $\mu$ L of fresh medium, containing DNCs in PBS at different gadolinium concentrations, was added in triplicate. The liquid was aspirated off after different incubation times and replaced with 100  $\mu$ L of fresh medium and 10  $\mu$ L of MTT reagent. After a 2 h incubation, 100  $\mu$ L of detergent reagent was added and the plate was swirled gently in the dark at room temperature for 2 h. The absorbance at 570 nm was measured in a microplate reader (Bio Tek Instruments, Inc.).

**Biodistribution Studies.** Female nu/nu nude mice were obtained from Charles River at 6 weeks of age. Mice ( $n = 3$ ) were anesthetized with isoflurane, and 59 nm polydisulfide DNCs were administered *via* tail vein injection at a gadolinium dose of 0.18 mmol/kg. The injected volume of contrast agent per mouse was 200  $\mu$ L. Blood was collected at 1, 2, 4, 6, and 24 h time points. The mice were sacrificed after 24 h, and organs of interest were harvested. Both blood and organ samples were analyzed by inductively coupled plasma mass spectroscopy (ICP-MS) to quantitatively determine the concentration of gadolinium. All ICP-MS measurements were performed by the New Bolton Center Toxicology Laboratory, University of Pennsylvania, School of Veterinary Medicine, Kennett Square, PA, USA, using an Elan 6100 ICP-MS (Perkin-Elmer, Shelton, CT, USA). Analogous animal studies ( $n = 3$ ) were performed with PAMAM(G3)-[Gd-C-DOTA] $^{-1}$ , using an equivalent Gd dose of 0.18 mmol/kg.

For each DNC/dendrimer formulation, the percent injected dose per gram of tissue (%I.D./g) was calculated as  $[\text{Ln}]_{\text{sample}}/([\text{Ln}]_{\text{inj}} \times M_{\text{inj}})$ , where  $[\text{Ln}]_{\text{sample}}$  is the Gd concentration in the sample (blood, tumor, or organ tissue),  $[\text{Ln}]_{\text{inj}}$  is the Gd concentration in the injected nanoparticle solution, and  $M_{\text{inj}}$  is the mass of the nanoparticle solution injected.

**Contrast-Enhanced *In Vivo* MR Imaging.** Approximately 6 week old female nu/nu nude mice ( $n = 3$ ; Charles River Laboratory, Charles River, MS) were maintained in accordance with the Institutional Animal Care and Use Committee (IACUC) of the University of Pennsylvania. Precontrast images were acquired using a 4.7 T small animal horizontal bore Varian INOVA system.  $T_1$ -weighted images were acquired in the coronal plane using parameters as follows: repetition time (TR) = 392 ms, echo time (TE) = 5.12 ms, FOV = 80  $\times$  40 mm, flip angle = 30°, slice thickness = 0.5 mm, number of requisition = 6, resolution = 256  $\times$  128 pixels. Immediately following the precontrast image acquisition, the polydisulfide DNCs or PAMAM(G3)-[Gd-C-DOTA] $^{-1}$  were administered *via* tail vein injection at gadolinium concentration of 0.18 mmol/kg. Postcontrast images were acquired at 15 min, 1 h, 2 h, 4 h, and 24 h under the same imaging parameters used for precontrast images.

**Image Analysis.** For quantitative analysis of MR images, the average MR signal intensities (SI) within operator-defined regions of interest encircling the tissue of interest and muscle were measured. The tissue-to-muscle (T/M) ratio was then calculated. The relative tissue-to-muscle (rT/M) ratio was calculated as the quotient of the T/M ratio in postcontrast images and precontrast images. A *t* test (two-tailed, unequal variance) was used to compare the rT/M at different time points postinjection. A  $p < 0.05$  was considered statistically significant.

**Conflict of Interest:** The authors declare no competing financial interest.

**Acknowledgment.** This research was supported in part by the National Institute of Health (NIH) NIBIB/R01-EB012065 (A.T.), NCI/R01-CA157766 (A.T.), NIBIB/R21-EB013226 (A.T.), and the Intramural Research Program of the NIH, National Cancer Institute, Center for Cancer Research (M.B.).

**Supporting Information Available:** Supplemental Figures S1–S6. This material is available free of charge *via* the Internet at <http://pubs.acs.org>.

## REFERENCES AND NOTES

- Caravan, P.; Ellison, J. J.; McMurry, T. J.; Lauffer, R. B. Gadolinium(III) Chelates as MRI Contrast Agents: Structure, Dynamics, and Applications. *Chem. Rev.* **1999**, *99*, 2293–2352.
- Lauffer, R. B. Paramagnetic Metal Complexes as Water Proton Relaxation Agents for NMR Imaging: Theory and Design. *Chem. Rev.* **1987**, *87*, 901–927.
- Duarte, M. G.; Gil, M. H.; Peters, J. A.; Colet, J. M.; Elst, L. V.; Muller, R. N.; Geraldes, C. F. G. C. Synthesis, Characterization, and Relaxivity of Two Linear Gd(DTPA)-Polymer Conjugates. *Bioconjugate Chem.* **2001**, *12*, 170–177.
- Kobayashi, H.; Brechbiel, M. W. Nano-Sized MRI Contrast Agents with Dendrimer Cores. *Adv. Drug Delivery Rev.* **2005**, *57*, 2271–2286.
- Cheng, Z.; Thorek, D. L. J.; Tsourkas, A. Porous Polymerosomes with Encapsulated Gd-Labeled Dendrimers as Highly Efficient MRI Contrast Agents. *Adv. Funct. Mater.* **2009**, *19*, 3753–3759.
- Cheng, Z.; Tsourkas, A. Paramagnetic Porous Polymerosomes. *Langmuir* **2008**, *24*, 8169–8173.
- Liebold, L.; Anderson, S.; Willits, D.; Oltrogge, L.; Frank, J. A.; Douglas, T.; Young, M. Viral Capsids as MRI Contrast Agents. *Magn. Reson. Med.* **2007**, *58*, 871–879.
- Vivero-Escoto, J. L.; Taylor-Pashow, K. M. L.; Huxford, R. C.; Della Rocca, J.; Okoruwa, C.; An, H.; Lin, W.; Lin, W. Multifunctional Mesoporous Silica Nanospheres with Cleavable Gd(III) Chelates as MRI Contrast Agents: Synthesis, Characterization, Target-Specificity, and Renal Clearance. *Small* **2011**, *7*, 3519–3528.



9. Barrett, T.; Kobayashi, H.; Brechbiel, M.; Choyke, P. L. Macromolecular MRI Contrast Agents for Imaging Tumor Angiogenesis. *Eur. J. Radiol.* **2006**, *60*, 353–366.
10. Bogdanov, A. A., Jr.; Weissleder, R.; Frank, H. W.; Bogdanova, A. V.; Nossif, N.; Schaffer, B. K.; Tsai, E.; Papisov, M. I.; Brady, T. J. A New Macromolecule as a Contrast Agent for MR Angiography: Preparation, Properties, and Animal Studies. *Radiology* **1993**, *187*, 701–706.
11. Brasch, R. C. Rationale and Applications for Macromolecular Gd-Based Contrast Agents. *Magn. Reson. Med.* **1991**, *22*, 282–287 discussion 300–303.
12. Kuo, P. H.; Kanal, E.; Abu-Alfa, A. K.; Cowper, S. E. Gadolinium-Based MR Contrast Agents and Nephrogenic Systemic Fibrosis. *Radiology* **2007**, *242*, 647–649.
13. Lu, Z. R.; Mohs, A. M.; Zong, Y.; Feng, Y. Polydisulfide Gd(III) Chelates as Biodegradable Macromolecular Magnetic Resonance Imaging Contrast Agents. *Int. J. Nanomed.* **2006**, *1*, 31–40.
14. Lu, Z.-R.; Wu, X. Polydisulfide-Based Biodegradable Macromolecular Magnetic Resonance Imaging Contrast Agents. *Isr. J. Chem.* **2010**, *50*, 220–232.
15. Haag, R. Supramolecular Drug-Delivery Systems Based on Polymeric Core-Shell Architectures. *Angew. Chem., Int. Ed.* **2004**, *43*, 278–282.
16. Deneke, S. M. Thiol-Based Antioxidants. *Curr. Top. Cell. Regul.* **2000**, *36*, 151–180.
17. Cheng, Z.; Thorek, D. L. J.; Tsourkas, A. Gadolinium-Conjugated Dendrimer Nanoclusters as a Tumor-Targeted  $T_1$  Magnetic Resonance Imaging Contrast Agent. *Angew. Chem., Int. Ed.* **2010**, *49*, 346–350.
18. Nwe, K.; Xu, H.; Regino, C. A. S.; Bernardo, M.; Ileva, L.; Riffle, L.; Wong, K. J.; Brechbiel, M. W. A New Approach in the Preparation of Dendrimer-Based Bifunctional Diethylenetriaminepentaacetic Acid MR Contrast Agent Derivatives. *Bioconjugate Chem.* **2009**, *20*, 1412–1418.
19. Gringeri, C. V.; Menchise, V.; Rizzitelli, S.; Cittadino, E.; Catanzaro, V.; Dati, G.; Chaabane, L.; Digilio, G.; Aime, S. Novel Gd(III)-Based Probes for MR Molecular Imaging of Matrix Metalloproteinases. *Contrast Media Mol. Imaging* **2012**, *7*, 175–184.
20. Jacques, V.; Dumas, S.; Sun, W. C.; Troughton, J. S.; Greenfield, M. T.; Caravan, P. High-Relaxivity Magnetic Resonance Imaging Contrast Agents. Part 2. Optimization of Inner- and Second-Sphere Relaxivity. *Invest. Radiol.* **2010**, *45*, 613–624.
21. Laurent, S.; Henoumont, C.; Vander Elst, L.; Muller, R. N. Synthesis and Physicochemical Characterisation of Gd-DTPA Derivatives as Contrast Agents for MRI. *Eur. J. Inorg. Chem.* **2012**, *2012*, 1889–1915.
22. Liu, Y.; Zhang, N. Gadolinium Loaded Nanoparticles in Theranostic Magnetic Resonance Imaging. *Biomaterials* **2012**, *33*, 5363–5375.
23. Reynolds, F.; O'Loughlin, T.; Weissleder, R.; Josephson, L. Method of Determining Nanoparticle Core Weight. *Anal. Chem.* **2005**, *77*, 814–817.
24. Sato, N.; Kobayashi, H.; Hiraga, A.; Saga, T.; Togashi, K.; Konishi, J.; Brechbiel, M. W. Pharmacokinetics and Enhancement Patterns of Macromolecular MR Contrast Agents with Various Sizes of Polyamidoamine Dendrimer Cores. *Magn. Reson. Med.* **2001**, *46*, 1169–1173.
25. Crayton, S. H.; Elias, D. R.; Al Zaki, A.; Cheng, Z.; Tsourkas, A. ICP-MS Analysis of Lanthanide-Doped Nanoparticles as a Non-radiative, Multiplex Approach To Quantify Biodistribution and Blood Clearance. *Biomaterials* **2012**, *33*, 1509–1519.
26. Langereis, S.; de Lussanet, Q. G.; van Genderen, M. H. P.; Meijer, E. W.; Beets-Tan, R. G. H.; Griffioen, A. W.; van Engelshoven, J. M. A.; Backes, W. H. Evaluation of Gd(III)-DTPA-Terminated Poly(propylene Imine) Dendrimers as Contrast Agents for MR Imaging. *NMR Biomed.* **2006**, *19*, 133–141.
27. Kobayashi, H.; Kawamoto, S.; Jo, S.-K.; Bryant, H. L.; Brechbiel, M. W.; Star, R. A. Macromolecular MRI Contrast Agents with Small Dendrimers: Pharmacokinetic Differences between Sizes and Cores. *Bioconjugate Chem.* **2003**, *14*, 388–394.
28. Sadekar, S.; Ray, A.; Janat-Amsbury, M.; Peterson, C. M.; Ghandehari, H. Comparative Biodistribution of PAMAM Dendrimers and HPMA Copolymers in Ovarian-Tumor-Bearing Mice. *Biomacromolecules* **2010**, *12*, 88–96.
29. Deo, A.; Fogel, M.; Cowper, S. E. Nephrogenic Systemic Fibrosis: A Population Study Examining the Relationship of Disease Development to Gadolinium Exposure. *Clin. J. Am. Soc. Nephrol.* **2007**, *2*, 264–267.
30. Morcos, S. K. Nephrogenic Systemic Fibrosis Following the Administration of Extracellular Gadolinium Based Contrast Agents: Is the Stability of the Contrast Agent Molecule an Important Factor in the Pathogenesis of this Condition? *Br. J. Radiol.* **2007**, *80*, 73–76.
31. Perazella, M. A. Nephrogenic Systemic Fibrosis, Kidney Disease, and Gadolinium: Is There a Link?. *Clin. J. Am. Soc. Nephrol.* **2007**, *2*, 200–202.
32. Penfield, J. G.; Reilly, R. F. Nephrogenic Systemic Fibrosis Risk: Is There a Difference between Gadolinium-Based Contrast Agents?. *Semin. Dial.* **2008**, *21*, 129–134.
33. Bousquet, J. C.; Saini, S.; Stark, D. D.; Hahn, P. F.; Nigam, M.; Wittenberg, J.; Ferrucci, J. T. Gd-DOTA: Characterization of a New Paramagnetic Complex. *Radiology* **1988**, *166*, 693–698.
34. Liu, M.; Fréchet, J. M. J. Designing Dendrimers for Drug Delivery. *Pharm. Sci. Technol. Today* **1999**, *2*, 393–401.
35. Zong, Y.; Wang, X.; Jeong, E.-K.; Parker, D. L.; Lu, Z.-R. Structural Effect on Degradability and *In Vivo* Contrast Enhancement of Polydisulfide Gd(III) Complexes as Biodegradable Macromolecular MRI Contrast Agents. *Magn. Reson. Imaging* **2009**, *27*, 503–511.
36. Ke, T.; Feng, Y.; Guo, J.; Parker, D. L.; Lu, Z.-R. Biodegradable Cystamine Spacer Facilitates the Clearance of Gd(III) Chelates in Poly(glutamic acid) Gd-DO3A Conjugates for Contrast-Enhanced MR Imaging. *Magn. Reson. Imaging* **2006**, *24*, 931–940.
37. Sarin, H. Physiologic Upper Limits of Pore Size of Different Blood Capillary Types and Another Perspective on the Dual Pore Theory of Microvascular Permeability. *J. Angiogenesis Res.* **2010**, *2*, 14.
38. Longmire, M.; Choyke, P. L.; Kobayashi, H. Clearance Properties of Nano-Sized Particles and Molecules as Imaging Agents: Considerations and Caveats. *Nanomedicine* **2008**, *3*, 703–717.
39. Nwe, K.; Bryant, L. H.; Brechbiel, M. W. Poly(amidoamine) Dendrimer Based MRI Contrast Agents Exhibiting Enhanced Relaxivities Derived via Metal Preligation Techniques. *Bioconjugate Chem.* **2010**, *21*, 1014–1017.
40. Nwe, K.; Bernardo, M.; Regino, C. A. S.; Williams, M.; Brechbiel, M. W. Comparison of MRI Properties between Derivatized DTPA and DOTA Gadolinium-Dendrimer Conjugates. *Bioorg. Med. Chem.* **2010**, *18*, 5925–5931.
41. Andersson, A.; Lindgren, A.; Hultberg, B. Effect of Thiol Oxidation and Thiol Export from Erythrocytes on Determination of Redox Status of Homocysteine and Other Thiols in Plasma from Healthy Subjects and Patients with Cerebral Infarction. *Clin. Chem.* **1995**, *41*, 361–366.